Fabrication and Characterization of Temperature Insensitive 660-nm Resonant-Cavity LEDs

Jun-Rong Chen, Tsung-Shine Ko, Tien-Chang Lu, *Member, IEEE*, Yi-An Chang, Hao-Chung Kuo, *Senior Member, IEEE*, Yen-Kuang Kuo, Jui-Yen Tsai, Li-Wen Laih, and Shing-Chung Wang, *Life Member, IEEE, Fellow, OSA*

***Abstract*—InGaP/AlGaInP 660-nm resonant-cavity light-emitting diodes (RCLEDs) with stable temperature characteristics have been achieved by extending the resonant cavity length from one optical wavelength (1λ) to three optical wavelengths (3λ) and tripling the number of quantum wells. When the operation temperature increases from 25 °C to 95 °C, the degree of power variation at 20 mA is reduced from −2.1 dB to −0.6 dB for the conventional 1-λ cavity RCLEDs and 3-λ cavity RCLEDs, respectively. In order to interpret the temperature-dependent experimental results, advanced device simulation is applied to model the RCLEDs with different cavity designs. According to the numerical simulation results, we deduce that the stable temperature-dependent output performance should originate from the reduction of electron leakage current and thermally enhanced hole transport for the 3-λ cavity AlGaInP RCLEDs.**

***Index Terms*—Leakage current, modeling, polymethyl methacrylate plastic optic fiber (POF), resonant-cavity light-emitting diode (RCLED), semiconductor device.**

I. Introduction

RESONANT-CAVITY light-emitting diodes (RCLEDs) have been adopted as ideal light sources for optical interconnects due to several inherent advantages including enhanced output intensities, narrow spectral linewidth, improved beam directionality, high modulation bandwidth, and thresholdless operation [1], [2]. Especially, RCLEDs operating at near 660 nm have become a key component for the application in short-distance data communication system due to a minimum attenuation loss of 0.15 dB/m at 650 nm in the polymethyl methacrylate plastic optical fibers (POFs) [3]. Conceptually, a typical RCLED consists of two distributed Bragg reflectors (DBRs) and an active layer located between two mirrors. In a conventional light-emitting diode (LED), only about 4% of light is escaped from the surface of LED due to the large refractive index of semiconductors. As compared to conventional LEDs, the resonant cavity of RCLED forces the light to emit into the radiation cone for a certain wavelength instead of isotropic emission. Furthermore, when the thickness of the resonant cavity is shortened to be only several optical wavelengths, the effect of photon quantization in this microcavity will enhance spontaneous emission properties. For more details about RCLEDs, the reader can refer to the related review paper [4].

Further applications of RCLEDs and POFs have been developed to the automotive industry, such as media oriented systems transport (MOST), which needs to carry 50–250 Mb/s of data over POFs. Therefore, higher temperature-stable output performance is required for AlGaInP RCLEDs applied in this field. One of the most important approaches to improve the temperature-dependent performance is the engineering of gain cavity resonance alignment. Specifically, the cavity mode is often intentionally designed to be at a slightly longer wavelength relative to the peak gain at room temperature. As the device is heated with the increasing injection current, the peak gain shifts into alignment with the cavity mode to provide optimum RCLED performance. However, the device temperature increases with increasing operating current. It can be expected that the RCLED output power is limited by the temperature-induced misalignment at higher operating temperatures. Consequently, the gain cavity alignment within an RCLED can be engineered to obtain low temperature-insensitive performance at a particular temperature range. Based on this engineering technology, Hild *et al.* reported the AlGaInP RCLEDs with a less temperature sensitivity over the temperature range from 15 °C to 75 °C by employing the design of a large gain cavity detuning [5]. Nevertheless, they found that the prevalence of electron leakage reduces the output efficiency with increasing operation temperature [5]–[7]. Furthermore, several high-performance AlGaInP RCLEDs have been reported in recent years. The demonstrated properties include high output power [8], high external quantum efficiency [9], low operation voltage [10], high emission directionality [11], and high modulation bandwidth [12]–[15]. Although significant progress in AlGaInP RCLEDs has been achieved under room temperature operation, it is still necessary to improve the temperature-dependent output performance as the injection current and operation temperature increase. As compared to

Manuscript received December 3, 2007; revised January 22, 2008. Published August 29, 2008 (projected).This work was supported by the MOE ATU program and in part by the National Science Council of the Republic of China under Contracts NSC 95-2120-M-009-008, NSC 95-2752-E-009-007-PAE, NSC 95-2221-E-009-282, and NSC 95-2112-M-018-007.

J.-R. Chen, T.-S. Ko, T.-C. Lu, H.-C. Kuo, and S.-C. Wang are with the Department of Photonics and Institute of Electro-Optical Engineering, National Chiao Tung University, Hsinchu 30050, Taiwan, R.O.C. (e-mail: jrchen.eo95g@nctu.edu.tw; tsko.eo93g@nctu.edu.tw; timtclu@faculty.nctu.edu.tw; hckuo@faculty.nctu.edu.tw; scwang@cc.nctu.edu.tw).

Y.-A. Chang was with the Department of Photonics and Institute of Electro-Optical Engineering, National Chiao Tung University, Hsinchu 30050, Taiwan, R.O.C.. He is now with the Millennium Communication Co., Ltd., Hsinchu 303, Taiwan, R.O.C. (e-mail: rayman0313.eo92g@nctu.edu.tw).

Y.-K. Kuo is with the Department of Physics, National Changhua University of Education, Changhua 50058, Taiwan, R.O.C. (e-mail: ykuo@cc.ncue.edu.tw).

J.-Y. Tsai and L.-W. Laih are with the Millennium Communication Co., Ltd., Hsinchu 303, Taiwan, R.O.C. (e-mail: jytsai@m-comm.com.tw; lwlaih@m-comm.com.tw).

Digital Object Identifier 10.1109/JLT.2008.920639

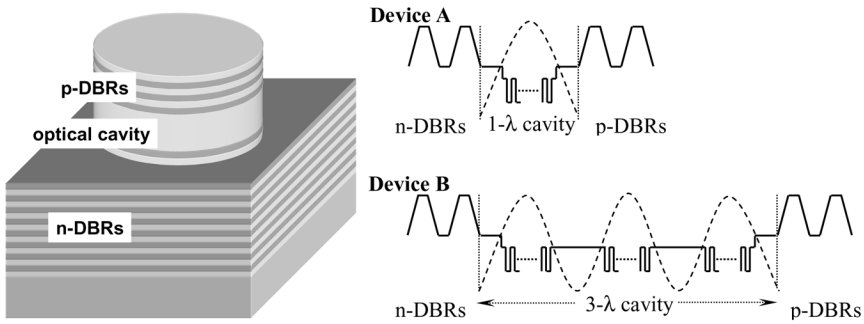

Fig. 1. Schematic plot of device structure. Device A is designed with a conventional 1-λ resonant cavity. Device B is designed to have a 3-λ resonant cavity, while the number of QWs is tripled and separated into three parts.

AlGaAs-based light emitters, AlGaInP-based light emitters have two major intrinsic drawbacks. One is the limited barrier height in the InGaP/AlGaInP heterostructure, and the other is the larger thermal resistivity, which is induced by the large mass difference between Ga and In [16]. Therefore, the temperature-induced efficiency degradation is more serious for AlGaInP-based light emitters.

In our previous study, we have demonstrated the AlGaInP 660-nm RCLEDs with the temperature insensitive output characteristics by extending the resonant cavity length from one optical wavelength to three optical wavelengths and tripling the number of quantum wells. The temperature-dependent light-current characteristics exhibited highly stable behavior with increasing operation temperature [17]. In order to further investigate the device physics of the RCLED devices, we present in this paper a theoretical analysis of the structure-dependent RCLED output characteristics by using advanced device simulation. We will focus on investigating how the device temperature affects the electron leakage current and the carrier concentration distribution for the RCLEDs with different designs of cavity structures. Moreover, the physical mechanism that leads to the results of temperature-insensitive light-current characteristics will be discussed as well.

II. Fabricated Device Characteristics

The AlGaInP RCLED structures in this specific study were grown by a low pressure (50 torr) Veeco D180 metal-organic chemical vapor deposition (MOCVD) system on n-type GaAs substrates. Methyl-organometallics, phosphine, and arsine were used as the sources for epitaxy. SiH_4, CBr_4, and DEZn were the n- and p-type dopants. A schematic plot of the RCLED structures is shown in Fig. 1. Two different structures were prepared, in which the bottom DBR identically consisted of 35 pairs of n-type quarter-wave $Al_{0.95}Ga_{0.05}As/Al_{0.5}Ga_{0.5}As$ layers for both devices to provide a $\sim$99% reflectivity. The top DBRs consisted of seven pairs of p-type $Al_{0.95}Ga_{0.05}As/Al_{0.5}Ga_{0.5}As$ layers. A separate-confinement-heterostructure strained multiple quantum wells (MQWs) active region, which contained $In_{0.52}Ga_{0.48}P$ wells and $(Al_{0.5}Ga_{0.5})_{0.5}In_{0.5}P$ barriers, and $(Al_{0.7}Ga_{0.3})_{0.5}In_{0.5}P$ cladding layers formed the resonant cavity. For device A, the thickness of optical cavity was standardized to 1λ and contained seven quantum wells at the antinode of the standing wave. As for device B, the thickness of optical cavity was extended to 3λ and the number of quantum wells was tripled as well. The doping levels of n- and p-type DBRs, determined from electrochemical capacitance-voltage (ECV) measurement, were 2×10^{18} and 4×10^{18} cm^{-3}, respectively. After epitaxial growth, standard fabrication processes, including photolithography, implantation, metallization, and bonding techniques, were used to fabricate these two RCLED devices. The light extraction window of both devices in this study was 80 μm in diameter. The RCLED chips were mounted onto TO-46 headers and the chip size was in 250×250 μm^2.

Fig. 2 shows the spectra of quantum-well photoluminescence and reflectivity spectra of devices A and B. In Fig. 2, it is found that the values of gain cavity detuning are about 8 and 11 nm for devices A and B, respectively. We will show later that this difference is not the main mechanism which causes the different device performances for devices A and B. Fig. 3 illustrates the temperature-dependent *L–I–V* characteristics of the fabricated devices A and B. The highly C-doped p-type DBRs and high-quality ohmic contacts result in a low operating voltage of 2.1 V at a current of 20 mA in device A, while the thicker undoped cavity in device B gives a higher voltage of 2.37 V. An output power of 1.9 mW in device A at 20 mA under room-temperature operation is achieved, and the maximum output power of 3.1 mW can be achieved as the input current is about 57 mA. For device B, even though the output power at low current injection is not higher than that of device A, the output characteristic shows more stable with increasing operation temperature, which indicates that the temperature-dependent effects on output performance of device B are not evident. The power variations between 25 °C and 95 °C at 20 mA for devices A and B are approximately -2.1 and -0.6 dB, respectively. Furthermore, although the maximum output power of device B is lower than that of device A at the operation temperature of 25 °C, it is found that when the operation temperature increases from 25 °C to 95 °C, device B can provide larger output power than device A. This result suggests that device B has better performance under high-temperature operation.

According to the aforementioned experimental results, it is found that although the maximum output power of device B is lower than that of device A at 25 °C, the decrease of output power of device B with increasing operation temperature is more subtle than that of device A. In the following investigation, we will employ theoretical simulation to understand the

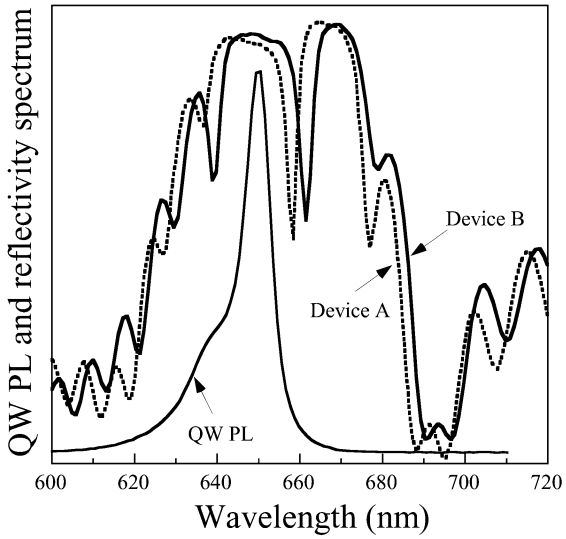

Fig. 2. Spectra of quantum well photoluminescence and reflectivity spectra of devices A and B.

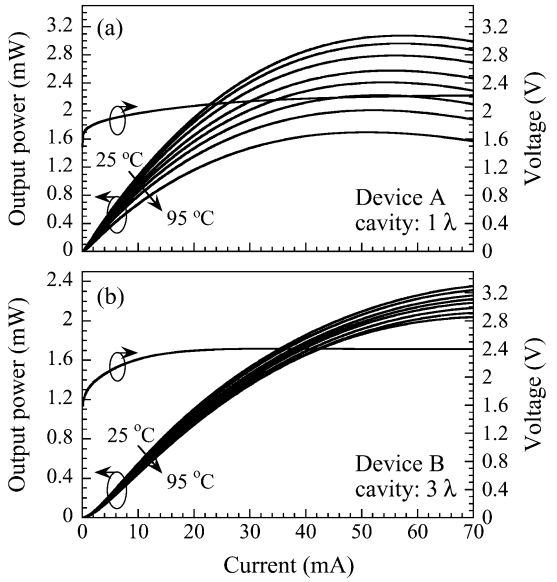

Fig. 3. Temperature-dependent *L–I–V* characteristic of (a) device A and (b) device B. The curve was obtained in a device temperature range of 25 °C–95 °C.

internal physical processes in these two RCLED devices and further analyze the origins of the improved temperature-dependent output characteristics for device B.

III. Theoretical Model

The numerical simulations in this study are performed by using an advanced physical model of semiconductor devices (APSYS) modeling software [18], which is based on 2-D/3-D finite-element analysis. The physical model self-consistently combines Poisson's equation, current continuity equations, carrier energy transport equations, heat transfer equations, conventional drift-diffusion equations, photon rate equations, and scalar wave equation. In the optical mode model, all modes are treated as possible since they all contribute to the noncoherent spontaneous emission power [19]. Photon recycling effect is rigorously taken into account by accurately determinate photon power density. The calculation of quantum-well band structure is based on the $k{\cdot}p$ theory with envelope function approximation [20]. Except for the bandgap energies, in order to obtain the numerical parameters required for $k{\cdot}p$ calculations for the AlGaInP materials, a linear interpolation among InP, GaP, and AlP is utilized in this study [21], [22]. The material parameters of the binary semiconductors used in this study are taken from the values reported by Vurgaftman *et al.* [23]. The formulas used in the calculation of unstrained AlGaInP bandgap energies are considered in accordance with the model provided by Mbaye *et al.* [24]. The temperature-dependent bandgap energies of the relevant binary semiconductors are calculated using the commonly employed Varshni formula and the Varshni parameters are taken from [23]. The conduction to valence band offset ratio is chosen as 65 : 35 according to the latest measurement results [25]. The spontaneous emission rate, with the valence-band-mixing effect being taken into account, could be expressed by [26]

$$r_{\rm sp}(E) = \frac{2nq^2E}{\pi^2\hbar^2c^3\varepsilon_0 m_0^2 L_z}\sum_{n,m} \times \int_0^\infty \frac{k_t M_{\rm nm}(k_t)\Gamma/(2\pi)}{\left(E_{\rm cn}(k_t) - E_{\rm kpm}(k_t) - E\right)^2 + (\Gamma/2)^2} \times f_c^n(1 - f_v^m)dk_t \quad (1)$$

where q is the free electron charge, h is the reduced Planck's constant, n is the refractive index, ε_0 is the free-space dielectric constant, c is the speed of light, L_z is the thickness of quantum well, E is the photon energy, $M_{\rm nm}\ (k_t)$ is the momentum matrix element in the strained quantum well, $\Gamma = \hbar/\tau$ is the broadening due to intraband scattering relaxation time τ, $E_{\rm cn}$ is the nth conduction subband, $E_{\rm kpm}$ is the mth valence subband from the $k{\cdot}p$ calculation, and f_c^n and f_v^m are the Fermi functions for the conduction band states and the valence band states, respectively. The indices n and m denote the electron states in the conduction band and the heavy hole (light hole) subband states in the valence band. To account for the broadening due to scattering, it is assumed that $\tau = 0.1$ ps during the calculations [27]–[29].

The effect of self-heating has a major impact on the performance of AlGaInP-based RCLED devices. The increase of internal temperature induced by current injection limits the maximum output power due to the increase of nonradiative carrier recombination, the spread of gain spectrum, and the temperature-induced gain-cavity misalignment at higher operation current. For the treatment of device heating, the thermoelectric power and thermal current induced by temperature gradient are considered by utilizing the methods provided by Wachutka *et al.* [30]. Various heat sources, including Joule heat, generation/recombination heat, Thomson heat, and Peltier heat, are taken into account in this specific study. The random distribution of alloy atoms in quaternary AlGaInP compounds causes strong alloy scattering of phonons, which leads to a significant reduction in the thermal conductivity. The thermal conductivity of quaternary alloys of the type $AB_xC_yD_{1-x-y}$ can be estimated from

binary values using [31]

$$\frac{1}{\kappa(x,y)} = \frac{x}{\kappa_{AB}} + \frac{y}{\kappa_{AC}} + \frac{1-x-y}{\kappa_{AD}} + xyC_{ABC} + x(1-x-y)C_{\mathrm{ABD}} + y(1-x-y)C_{\mathrm{ACD}} \quad (2)$$

with the empirical bowing parameters C_{ABC}, C_{ABD}, and C_{ACD}. In our calculation, the thermal conductivities of the binary AlP, GaP, and InP are 1.3, 0.77, and 0.68 W/Kcm, respectively [31], [32]. The empirical bowing parameters of AlGaP, AlInP, and GaInP are 30, 77, and 19.9 Kcm/W, respectively [31], [32].

The calculation of carrier capture and escape from the quantum wells is considered in accordance with the model provided by Romero *et al.* [33]. As for the calculation of refractive index, Adachi model is employed to calculate the refractive index values of the AlGaInP materials [34]. More descriptions about the physical models employed in APSYS simulation program, which is a useful tool to access new designs or to optimize existing devices, can be found in [31], [35], and [36].

IV. Simulation Results and Discussion

In order to interpret the temperature-dependent experimental results, we numerically model the AlGaInP-based RCLED structures, which include the active regions and DBRs in accordance with the experimental device structures. Device A (1-λ cavity) and device B (3-λ cavity) are numerically modeled to investigate the internal physical mechanism. All physical parameters and device structures are the same for these two RCLED structures except for the number of quantum wells and the optical thickness of resonant cavity. Fig. 4 shows the vertical profile of refractive index and optical intensity for devices A [Fig. 4(a)] and B [Fig. 4(b)]. For device A, the quantum wells are placed in the antinode position of the cavity standing wave, which can enhance the spontaneous emission and photon recycling in the microcavity-based system [37], [38]. As for the design of device B, the 21 pairs of quantum wells are separated into three parts and each part is individually placed in the antinode position of the cavity standing wave, as shown in Fig. 4(b). The simulation results of temperature-dependent light-current characteristics of devices A and B are shown in Fig. 5. It is clearly seen that the simulation results are approximately in agreement with experimental results. The temperature-insensitive light-current characteristics of device B are also obtained from the numerical calculations. Furthermore, the output properties as indicated in Fig. 5 are consistent with the experimental results, showing that the output power of device B is lower than that of device A at 25 °C and it is opposite at 95 °C. We will discuss and analyze the internal physical mechanisms in the following content.

As previously mentioned, the temperature-dependent performance of AlGaInP-based light emitters, such as laser diodes, LEDs, and RCLEDs is poor due to the limited barrier height in quantum wells and larger thermal resistivity. These two intrinsic drawbacks significantly enhance electron carrier leakage from active layers to the p-type layer, therefore accelerating the degradation of the device performance as the operation temperature and injection current increase [5]–[7], [16], [39]–[41]. Several methods have been proposed to suppress the leakage current, such as increasing p-type doping concentration to increase the barrier height [42], [43], employing the multiquantum barrier (MQB) structure to block the overflowing electrons [44], and utilizing the graded-index separate confinement heterostructure (GRIN-SCH) to reduce leakage current [45]. In this study, by extending the optical thickness of resonant cavity and tripling the number of quantum wells,

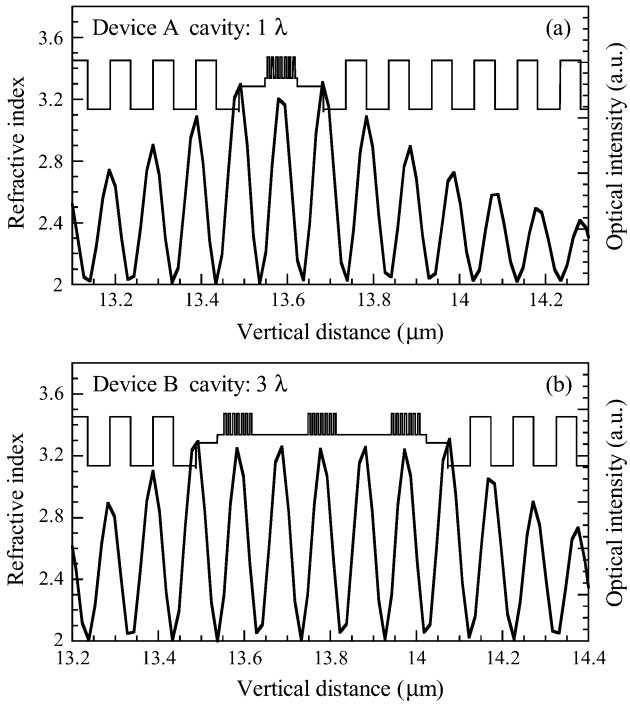

Fig. 4. Vertical profile of refractive index and optical intensity for (a) device A and (b) device B.

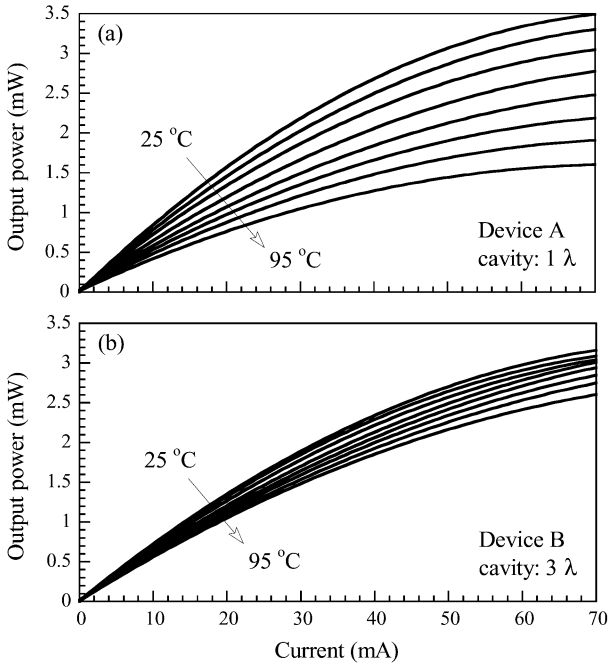

Fig. 5. Numerical results of temperature dependent *L–I* characteristics of (a) device A and (b) device B.

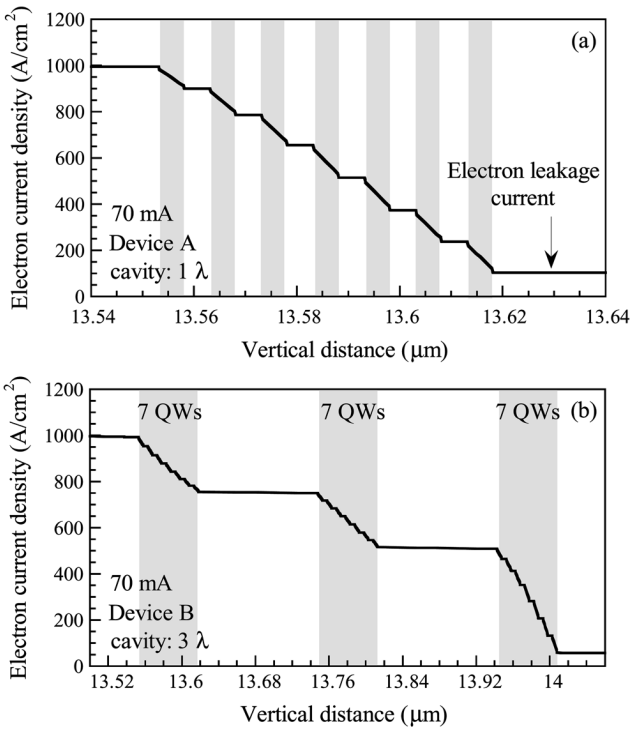

Fig. 6. Vertical electron current distribution at the injection current of 70 mA within the active regions of (a) device A and (b) device B.

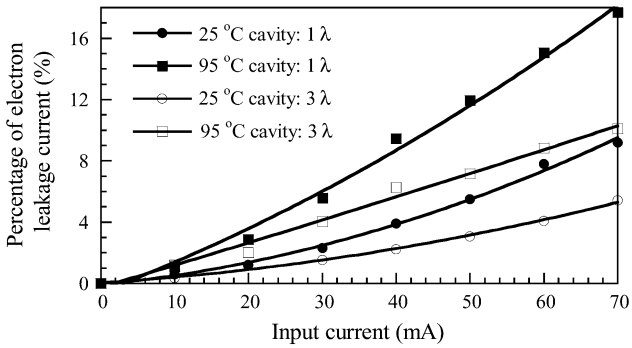

Fig. 7. Percentage of electron leakage current as a function of the bias current in devices A and B when the device temperatures are 25 °C and 95 °C, respectively.

we have observed that the effect of electron leakage current can be efficiently suppressed. In order to discuss the effect of electron leakage current in these two devices, the vertical electron current distributions within the active regions at 70 mA injection current are plotted in Fig. 6. The positions of quantum wells are marked with gray areas. The left-hand side of this figure is the n-side of the devices. Electrons are injected from n-type layers into quantum wells and recombine with holes within quantum wells. Therefore, the electron current density decreases within the quantum wells gradually as the well position is close to the p-side, as shown in Fig. 6. For device A, it is observed that a considerable portion of electrons escapes from the quantum wells into the p-side, which lowers the recombination efficiency and prevents carriers from radiative recombination within quantum wells. As for device B, by increasing the number of quantum wells, less electron leakage current is observed, as shown in Fig. 6(b). Moreover, it is noteworthy that the seven quantum wells which are close to the p-side dominate carrier recombination. This condition can be found from the degree of reduction of electron current density in Fig. 6(b). We will show later that this phenomenon is attributed to the nonuniform distribution of hole carriers.

To further quantitatively analyze the effect of electron leakage current, the percentage of electron leakage current as a function of the bias current for devices A and B is plotted in Fig. 7 when the operation temperatures are 25 °C and 95 °C, respectively. The percentage of electron leakage current is defined as the ratio of the electron current overflowed to the p-type layer to that injected into the active region of the RCLED devices. As indicated in Fig. 7, the percentage of electron leakage current increases with increasing input current and operation temperature. By comparing the leakage current of devices A and B at 25 °C, it is found that the percentage of electron leakage current of device A is about twice larger than that of device B when the input current is 70 mA. Furthermore, as the operation temperature increases from 25 °C to 95 °C, the percentage of electron leakage current of device A becomes more severe than that of device B. Consequently, according to the numerical analysis of electron leakage current, it is found that electron leakage current can be significantly inhibited by extending the optical thickness of resonant cavity and increasing the number of quantum wells. Fig. 8 shows the schematic representation about the relation between electron leakage and quantum-well numbers. The increase of quantum-well number provides better electron confinement, especially for high temperature operation and high current injection. The rising device temperature at higher current injection would induce more leakage current, which results in less radiative recombination, and therefore decreases the output power. We consider that it is one of the most important roles, which result in the temperature-insensitive light-current characteristics for device B.

Although the increase of the number of quantum wells can decrease the percentage of electron leakage current, hole carrier transport in multiple-quantum-well active region from the p-side to the n-side is relatively difficult due to the larger effective mass and lower hole mobility as compared with electrons. Therefore, it is worth noting that more number of quantum wells may lead to nonuniform hole concentration distribution within multiple-quantum-well active region. Since the number of quantum wells increases from seven to 21 for device B, it is necessary to consider this issue. Fig. 9 shows the vertical profiles of the electron-hole recombination rate of device A at 25 °C and 95 °C, respectively, when the input current is 70 mA. By comparing Fig. 9(a) and (b), the decrease of spontaneous emission rate is about one-third of the total value as the operation temperature increases from 25 °C to 95 °C. Fig. 10 shows the vertical profiles of the electron-hole recombination rate of device B at 25 °C and 95 °C, respectively, when the input current is 70 mA. In Fig. 10(a), it is obvious that the spontaneous emission rate in 21 quantum wells is substantially nonuniform. However, when the operation temperature increases from 25 °C to 95 °C, relatively uniform spontaneous emission rate within active region

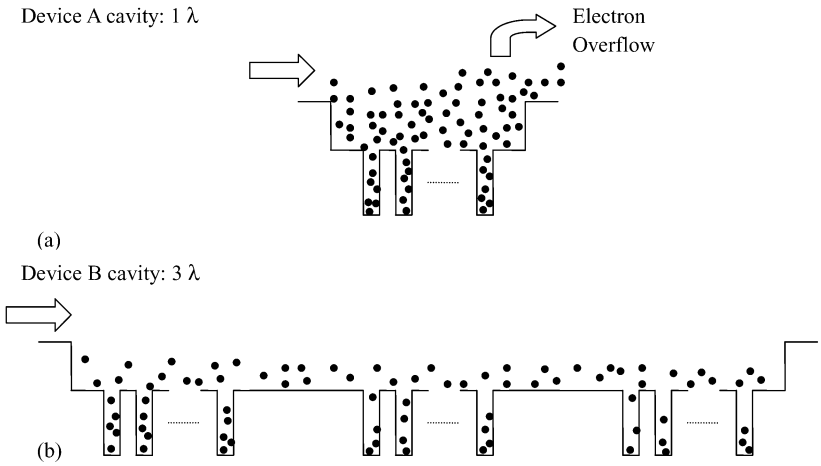

Fig. 8. Schematic representation about the relation between electron leakage and quantum-well numbers for (a) device A and (b) device B.

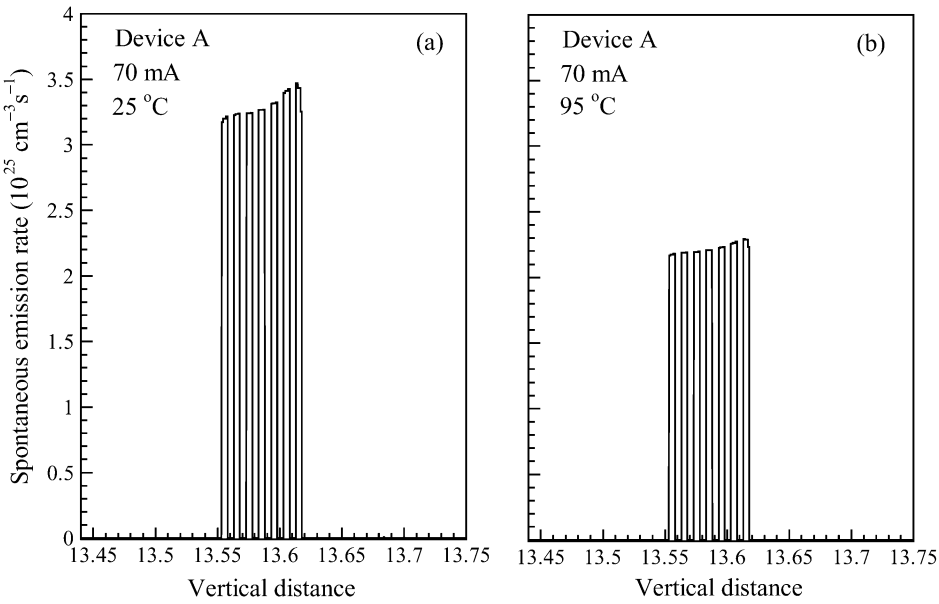

Fig. 9. Vertical profiles of the electron-hole recombination rate of device A at (a) 25 °C and (b) 95 °C.

is observed, as indicated in Fig. 10(b). Furthermore, the temperature-induced decrease of spontaneous emission rate is not serious for device B. This temperature-insensitive property for device B is consistent with previous light-current characteristics.

Recently, Ryu *et al.* investigated highly stable temperature characteristics of InGaN blue laser diodes [46] and found that thermally enhanced hole transport from the p-side to the n-side quantum well results in the enhancement of device performance and compensates temperature-induced losses when the device temperature increases. Since the number of quantum wells of device B is 21, hole transport in the multiple-quantum-well region may be another important role for device performance. In order to further study this effect, vertical profiles of hole concentration distribution within active region for device B are plotted in Fig. 11 as the operation temperatures are 25 °C and 95 °C, respectively. At 25 °C, hole concentration at the p-side quantum well is higher than that at the n-side quantum well due to the poor hole mobility and more number of quantum wells. Therefore, the vertical profile of spontaneous emission rate at 25 °C also shows the same distribution, as shown in Fig. 10(a). Moreover, when the number of quantum wells increases from seven to 21, the injected carriers spatially spread in these quantum wells, which results in lower carrier concentration in each quantum well and nonuniform carrier distribution. Therefore, the spontaneous emission rate and output power of device B are lower than that of device A when the operation temperature is 25 °C. On the contrary, as operation temperature increases, the hole concentration at the n-side quantum well increases as well. This mechanism originates from thermally enhanced hole transport from the p-side to the n-side quantum well, which leads to the increase in spontaneous emission rate at the n-side quantum well with increasing temperature, as shown in Fig. 10(b). Moreover, the hole concentration at the p-side quantum well does not increase obviously with temperature. Therefore, the decrease of spontaneous emission rate at the p-side quantum well is relatively larger than that at the n-side quantum well when the operation temperature increases from 25 °C to 95 ° C, as indicated in

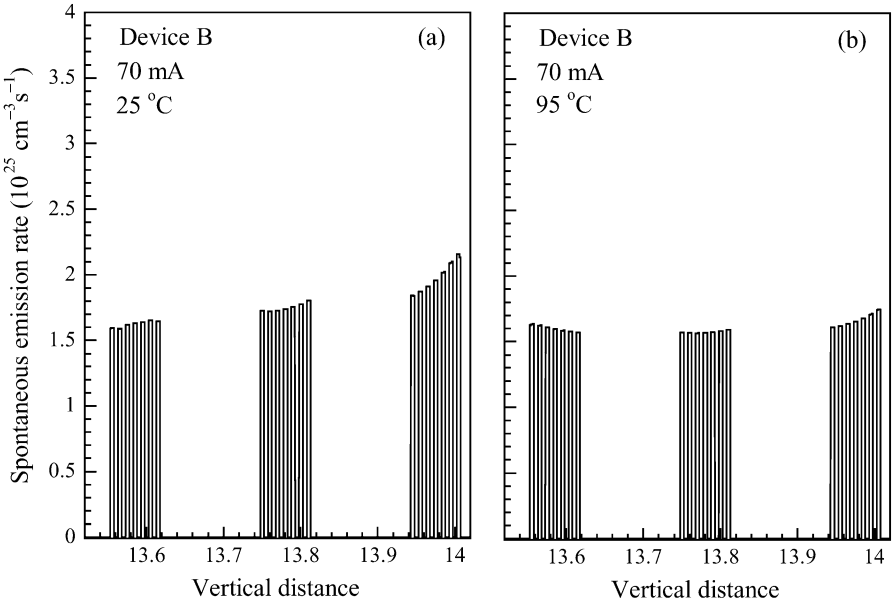

Fig. 10. Vertical profiles of the electron-hole recombination rate of device B at (a) 25 °C and (b) 95 °C.

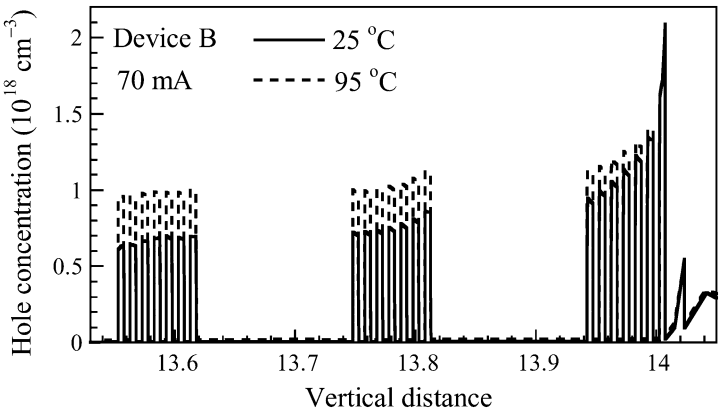

Fig. 11. Vertical profiles of hole concentration distribution within active region at the operation temperatures of 25 °C and 95 °C, respectively.

Fig. 10. This situation leads to the improved spontaneous emission rate and output power for device B under the operation temperature of 95 °C. Nevertheless, the hole concentration distribution within the multiple quantum wells is closely related to the depth and width of the quantum wells, the height of barrier, and the number of quantum wells. Consequently, in addition to the effect of electron leakage current, the temperature dependence of light-current characteristics should be still dependent on the design of active region.

V. Conclusion

We have numerically investigated how the device temperature affects the electron leakage current and the carrier concentration distribution for the RCLEDs with different designs of cavity structures. For conventional 1-λ cavity RCLEDs, electron leakage current is the main mechanism, which limits the output characteristics at elevated temperature. By extending the resonant cavity length from one optical wavelength to three optical wavelengths and tripling the number of quantum wells, the 3-λ cavity RCLEDs show highly stable temperature-dependent light-current characteristics. According to the numerical simulation results, it is found that the stable temperature-dependent light-current characteristics could originate from the reduction of electron leakage current and the thermally enhanced hole transport in multiple quantum wells. The optimization of InGaP/AlGaInP multiple quantum well structures would provide higher output power and improved temperature characteristics of AlGaInP-based RCLEDs.

Acknowledgment

The authors would like to thank the Crosslight incorporation for providing the advanced APSYS simulation program.

References

[1] M. M. Dumitrescu, M. J. Saarinen, M. D. Guina, and M. V. Pessa, "High-speed resonant cavity light-emitting diodes at 650 nm," *IEEE J. Sel. Topics Quantum Electron.*, vol. 8, no. 2, pp. 219–230, Mar./Apr. 2002.

[2] E. F. Schubert, *Light-Emitting Diodes*. Cambridge, U.K.: Cambridge Univ. Press, 2006, ch. 15.

[3] T. Ishigure, M. Satoh, O. Takanashi, E. Nihei, T. Nyu, S. Yamazaki, and Y. Koike, "Formation of the refractive index profile in the graded index polymer optical fiber for gigabit data transmission," *J. Lightw. Technol.*, vol. 15, no. 11, pp. 2095–2100, Nov. 1997.

[4] D. Delbeke, R. Bockstaele, P. Bienstman, R. Baets, and H. Benisty, "High-efficiency semiconductor resonant-cavity light-emitting diodes: A review," *IEEE J. Sel. Topics Quantum Electron.*, vol. 8, no. 2, pp. 189–206, Mar./Apr. 2002.

[5] K. Hild, T. E. Sale, T. J. C. Hosea, M. Hirotana, Y. Mizuno, and T. Kato, "Spectral and thermal properties of red AlGaInP RCLEDs for polymer optical fiber applications," *Inst. Electr. Eng. Proc.—Optoelectron.*, vol. 148, no. 5/6, pp. 220–224, 2001.

[6] A. I. Onischenko, T. E. Sale, E. P. O'Reilly, A. R. Adams, S. M. Pinches, J. E. F. Frost, and J. Woodhead, "Progress in the design and development of AlGaInP visible VCSELs," *Inst. Electr. Eng. Proc.—Optoelectron.*, vol. 147, no. 1, pp. 15–21, 2000.

[7] K. Streubel, N. Linder, R. Wirth, and A. Jaeger, "High brightness AlGaInP light-emitting diodes," *IEEE J. Sel. Topics Quantum Electron.*, vol. 8, no. 2, pp. 321–332, Mar./Apr. 2002.

[8] K. Streubel, U. Helin, V. Oskarsson, E. Bäcklin, and Å. Johansson, "High brightness visible (660 nm) resonant-cavity light-emitting diode," *IEEE Photon. Technol. Lett*, vol. 10, no. 12, pp. 1685–1687, Dec. 1998.

[9] R. Wirth, C. Karnutsch, S. Kugler, and K. Streubel, "High efficiency resonant-cavity LEDs emitting at 650 nm," *IEEE Photon. Technol. Lett*, vol. 13, no. 5, pp. 421–423, May 2001.

[10] J. W. Gray, Y. S. Jalili, P. N. Stavrinou, M. Whitehead, G. Parry, A. Joel, R. Robjohn, R. Petrie, S. Hunjan, P. Gong, and G. Duggan, "High-efficiency, low voltage resonant-cavity light-emitting diodes operating around 650 nm," *Electron. Lett.*, vol. 36, no. 20, pp. 1730–1731, 2000.

[11] R. Joray, M. Ilegems, R. P. Stanley, W. Schmid, R. Butendeich, R. Wirth, A. Jaeger, and K. Streubel, "Far-field radiation pattern of red emitting thin-film resonant cavity LEDs," *IEEE Photon. Technol. Lett*, vol. 18, no. 9, pp. 1502–1504, Sep. 2006.

[12] P. Sipilä, M. Saarinen, M. Guina, V. Vilokkinen, M. Toivonen, and M. Pessa, "Temperature behavior of resonant cavity light-emitting diodes at 650 nm," *Semicond. Sci. Technol.*, vol. 15, pp. 418–421, 2000.

[13] E. F. Schubert, N. E. J. Hunt, R. J. Malik, M. Micovic, and D. L. Miller, "Temperature and modulation characteristics of resonant-cavity light-emitting diodes," *J. Lightw. Technol.*, vol. 14, no. 7, pp. 1721–1729, Jul. 1996.

[14] M. Guina, S. Orsila, M. Dumitrescu, M. Saarinen, P. Sipilä, V. Vilokkinen, B. Roycroft, P. Uusimaa, M. Toivonen, and M. Pessa, "Light-emitting diode emitting at 650 nm with 200-MHz small-signal modulation bandwidth," *IEEE Photon. Technol. Lett.*, vol. 12, no. 7, pp. 786–788, Jul. 2000.

[15] C.-L. Tsai, C.-W. Ho, C.-Y. Huang, F.-M. Lee, M.-C. Wu, H.-L. Wang, S.-C. Ko, W.-J. Ho, J. Huang, and J. R. Deng, "Fabrication and characterization of 650 nm resonant-cavity light-emitting diodes," *J. Vac. Sci. Technol. B., Microelectron. Process. Phenom.*, vol. 22, no. 5, pp. 2518–2521, 2004.

[16] M.-F. Huang, M.-L. Tsai, J.-Y. Shin, Y.-L. Sun, R.-M. Yang, and Y.-K. Kuo, "Optimization of active layer structures to minimize leakage current for an AlGaInP laser diode," *Appl. Phys. A, Solids Surf.*, vol. 81, pp. 1369–1373, 2005.

[17] Y. A. Chang, C. L. Yu, I. T. Wu, H. C. Kuo, T. C. Lu, F. I. Lai, L. W. Laih, L. H. Laih, and S. C. Wang, "Design and fabrication of temperature-insensitive InGaP-InGaAlP resonant-cavity light-emitting diodes," *IEEE Photon. Technol. Lett.*, vol. 18, no. 16, pp. 1690–1692, Aug. 2006.

[18] APSYS Version 2006.7 Crosslight Software, Burnaby, BC, Canada, 2006.

[19] C. H. Henry, "Theory of spontaneous emission noise in open resonators and its application to lasers and optical amplifiers," *J. Lightw. Technol.*, vol. LT-4, no. 3, pp. 288–297, Mar. 1986.

[20] Y.-P. Chao and S. L. Chuang, "Spin-orbit-coupling effects on the valence-band structure of strained semiconductor quantum wells," *Phys. Rev. B., Condens. Matter*, vol. 46, pp. 4110–4122, 1992.

[21] J. Minch, S. H. Park, T. Keating, and S. L. Chuang, "Theory and experiment of $In_{1-x}Ga_xAs_yP_{1-y}$ and $In_{1-x-y}Ga_xAl_yAs$ long-wavelength strained quantum-well lasers," *IEEE J. Quantum Electron.*, vol. 35, no. 5, pp. 771–782, May 1999.

[22] S. T. Yen and C.-P. Lee, "Theoretical analysis of 630-nm band GaInP-AlGaInP strained quantum-well lasers considering continuum states," *IEEE J. Quantum Electron.*, vol. 33, no. 3, pp. 443–456, Mar. 1997.

[23] I. Vurgaftman, J. R. Meyer, and L. R. Ram-Mohan, "Band parameters for III-V compound semiconductors and their alloys," *J. Appl. Phys.*, vol. 89, pp. 5815–5875, 2001.

[24] A. A. Mbaye, C. Verié, and F. Aymerich, "Electronic structure of trimetallic III-V alloys: The Al1-x-zGaxInzP system," *Phys. Rev. B., Condens. Matter*, vol. 29, pp. 3756–3758, 1984.

[25] K. Interholzinger, D. Patel, C. S. Menoni, P. Thiagarajan, G. Y. Robinson, and J. E. Fouquet, "Strain-induced modifications of the band structure of $In_xGa_{1-x}P$-$In_{0.5}Al_{0.5}P$ multiple quantum wells," *IEEE J. Quantum Electron.*, vol. 34, no. 1, pp. 93–100, Jan. 1998.

[26] S. L. Chuang, *Physics of Optoelectronic Devices*. New York: Wiley, 1995.

[27] S. Kamiyama, T. Uenoyama, M. Mannoh, Y. Ban, and K. Ohnaka, "Analysis of GaInP/AlGaInP compressive strained multiple-quantum-well laser," *IEEE J. Quantum Electron.*, vol. 30, no. 6, pp. 1363–1369, Jun. 1994.

[28] S. Kamiyama, T. Uenoyama, M. Mannoh, and K. Ohnaka, "Theoretical studies of GaInP-AlGaInP strained quantum-well lasers including spin-orbit split-off band effect," *IEEE J. Quantum Electron.*, vol. 31, no. 8, pp. 1409–1417, Aug. 1995.

[29] S. Kamiyama, T. Uenoyama, M. Mannoh, Y. Ban, and K. Ohnaka, "Theoretical analysis of valence subband structures and optical gain of GaInP/AlGaInP compressive strained-quantum wells," *IEEE Photon. Technol. Lett.*, vol. 5, no. 4, pp. 439–441, Apr. 1993.

[30] G. K. Wachutka, "Rigorous thermodynamic treatment of heat generation and conduction in semiconductor device modeling," *IEEE Trans. Comput.-Aided Design Integr. Circuits Syst.*, vol. 9, no. 11, pp. 1141–1149, Nov. 1990.

[31] J. Piprek, *Semiconductor Optoelectronic Devices: Introduction to Physics and Simulation.*. San Diego, CA: Academic, 2003.

[32] W. Nakwaski, "Thermal conductivity of binary, ternary, and quaternary III-V compounds," *J. Appl. Phys.*, vol. 64, pp. 159–166, 1988.

[33] B. Romero, J. Arias, I. Esquivias, and M. Cada, "Simple model for calculating the ratio of the carrier capture and escape times in quantum-well lasers," *Appl. Phys. Lett.*, vol. 76, pp. 1504–1506, 2000.

[34] H. Kato, S. Adachi, H. Nakanishi, and K. Ohtsuka, "Optical properties of $(Al_xGa_{1-x})_{0.5}In_{0.5}P$ quaternary alloys," *Jpn. J. Appl. Phys.*, vol. 33, pp. 186–192, 1994.

[35] J. Piprek and S. Li, "GaN-based light emitting diodes," in *Optoelectronic Devices: Advanced Simulation and Analysis*. New York: Springer-Verlag, 2005.

[36] Y.-K. Kuo, S.-H. Yen, and J.-R. Chen, "Ultraviolet light-emitting diodes," in *Nitride Semiconductor Devices: Principles and Simulation*. New York: Wiley-VCH Verlag GmbH & Co. KGaA, 2007.

[37] G. Björk, S. Machida, Y. Yamamoto, and K. Igeta, "Modification of spontaneous emission rate in planar dielectric microcavity structures," *Phys. Rev. A., Gen. Phys.*, vol. 44, pp. 669–681, 1991.

[38] H. Benisty, H. D. Neve, and C. Weisbuch, "Impact of planar microcavity effects on light extraction—Part II: Selected exact simulations and role of photon recycling," *IEEE J. Quantum Electron.*, vol. 34, no. 9, pp. 1632–1643, Sep. 1998.

[39] D. P. Bour, D. W. Treat, R. L. Thornton, R. S. Geels, and D. F. Welch, "Drift leakage current in AlGaInP quantum-well lasers," *IEEE J. Quantum Electron.*, vol. 29, no. 5, pp. 1337–1343, May 1993.

[40] S. A. Wood, P. M. Smowton, C. H. Molloy, P. Blood, D. J. Somerford, and C. C. Button, "Direct monitoring of thermally activated leakage current in AlGaInP laser diodes," *Appl. Phys. Lett.*, vol. 74, pp. 2540–2542, 1999.

[41] P. Altieri, A. Jaeger, R. Windisch, N. Linder, P. Stauss, R. Oberschmid, and K. Streubel, "Internal quantum efficiency of high-brightness AlGaInP light-emitting devices," *J. Appl. Phys.*, vol. 98, p. 086101, 2005.

[42] G.-I. Hatakoshi, K. Itaya, M. Ishikawa, M. Okajima, and Y. Uematsu, "Short-wavelength InGaAlP visible laser diodes," *IEEE J. Quantum Electron.*, vol. 27, no. 6, pp. 1476–1482, Jun. 1991.

[43] G. J. Bauhuis, R. R. Hageman, and P. K. Larsen, "Heavily doped p-type AlGaInP grown by metalorganic chemical vapor deposition," *J. Crystal Growth.*, vol. 191, pp. 313–318, 1998.

[44] A. Sobiesierski, I. C. Sandall, P. M. Smowton, P. Blood, A. B. Krysa, M. R. Brown, K. S. Teng, and S. P. Wilks, "AlGaInP laser diodes incorporating a $3\lambda/4$ multiple quantum barrier," *Appl. Phys. Lett.*, vol. 86, p. 021102, 2005.

[45] M.-F. Huang, M.-L. Tsai, and Y.-K. Kuo, "Improvement of characteristic temperature for AlGaInP laser diodes," *Proc. SPIE—Int. Soc. Opt. Eng.*, vol. 5628, pp. 127–134, 2005.

[46] H. Y. Ryu, K. H. Ha, S. N. Lee, T. Jang, H. K. Kim, J. H. Chae, K. S. Kim, K. K. Choi, J. K. Son, H. S. Paek, Y. J. Sung, T. Sakong, O. H. Nam, and Y. J. Park, "Highly stable temperature characteristics of InGaN blue laser diodes," *Appl. Phys. Lett.*, vol. 89, p. 031122, 2006.

Jun-Rong Chen was born in Taichung, Taiwan, R.O.C., on October 23, 1980. He received the B.S. degree in physics from the National Changhua University of Education (NCUE), Changhua, Taiwan, R.O.C., in 2004 and the M.S. degree in optoelectronics from the Institute of Photonics, NCUE, Taiwan, R.O.C., in 2006. He is currently working towards the Ph.D. degree in the Department of Photonics and Institute of Electro-Optical Engineering, National Chiao Tung University (NCTU), Hsinchu, Taiwan, R.O.C.

He joined the Semiconductor Laser Technology Laboratory at NCTU in 2006, where he was engaged in research on III–V semiconductor materials for light-emitting diodes and semiconductor lasers under the instruction of Prof. T.-C. Lu, Prof. H.-C. Kuo, and Prof. S.-C. Wang. His recent research interests include III-nitride semiconductor lasers, epitaxial growth of III-nitride materials, and numerical simulation of III–V optoelectronic devices.

Tsung-Shine Ko was born in Tainan, Taiwan, R.O.C., in 1978. He received the B.S. degree in physics from the National Changhua University, Changhua, Taiwan, in 2001 and the M.S. degree in atomic science from the National Tsing Hau University, Hsinchu, Taiwan, in 2004. Since 2004, he has been working towards the Ph.D. degree in the Department of Photonics and Institute of Electro-Optical Engineering, National Chiao Tung University (NCTU), Hsinchu, Taiwan, R.O.C.

He was engaged in research on design of masks for extreme ultraviolet (EUV), the synthesis of gold nanoparticles and the growth of Si/Ge nanostructures under the instruction of Dr. J. Shieh, Prof. H. L. Chen, and Prof. T. C. Chu. His recent research interests include fabrication of nanostructure oxide materials and epitaxial growth of nonpolar GaN-based materials under the instruction of Prof. T. C. Lu, Prof. H. C. Kuo, and Prof. S. C. Wang. He will join Prof. J. Han's group at Yale University during 2008–2009 and mainly engage in further topics related to nitride-based materials and devices.

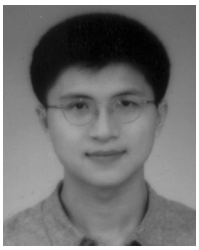

Tien-Chang Lu (M'07) received the B.S. degree in electrical engineering from the National Taiwan University, Taipei, Taiwan, R.O.C., in 1995, the M.S. degree in electrical engineering from the University of Southern California, Los Angeles, in 1998, and the Ph.D. degree in electrical engineering and computer science from the National Chiao Tung University, Hsinchu, Taiwan, R.O.C., in 2004.

He was with the Union Optronics Corporation as a Manager of Epitaxy Department in 2004. Since August 2005, he has been with the National Chiao Tung University as a member of the faculty in the Department of Photonics. His research work included the design, epitaxial growth, process, and characterization of optoelectronic devices, such as Fabry–Pérot-type semiconductor lasers, vertical-cavity surface-emitting lasers, resonant-cavity light-emitting diodes (LEDs), wafer-fused flip-chip LEDs, solar cells, etc. He has been engaged in the low-pressure MOCVD epitaxial technique associated with various material systems including InGaAlAs, InGaAsP, AlGaAs, InGaAlP, and InGaAlN, as well as the corresponding process skills. He is also interested in the structure design and simulations for optoelectronic devices using computer-aided software.

Yi-An Chang was born in Taipei, Taiwan, R.O.C., on March 13, 1978. He received the B.S. and M.S. degrees in physics from National Changhua University of Education (NCUE), Taiwan, R.O.C., in 2001 and 2003, respectively. From 2003 to 2007, he studied and received the Ph.D. degree in the Department of Photonics and Institute of Electro-Optical Engineering, National Chiao-Tung University. Under the instruction of Prof. H.-C. Kuo and Prof. S.-C. Wang, his research included the MOCVD epitaxial technology and the relevant process, and the theoretical simulation in the fabrication and analysis for III-nitride semiconductor devices, visible red InGaP/InGaAlP resonant-cavity LEDs, and infrared 850-nm VCSELs.

He joined the Laboratory of Lasers and Optical Semiconductors at NCUE in 2000 where he was engaged in research on passive Q-switching with solid-state saturable absorbers and III-nitride semiconductor materials for light-emitting diodes and semiconductor lasers under the instruction of Prof. Y.-K. Kuo. In 2008, he joined the Millennium Communication Co., Ltd., Hsinchu, Taiwan, R.O.C., where he is responsible for developing high-conversion-efficiency III–V compound solar cells.

Hao-Chung Kuo (S'98–M'99–SM'06) received the B.S. degree in physics from the National Taiwan University, Taipei, Taiwan, R.O.C., in 1990, the M.S. degree in electrical and computer engineering from Rutgers University, Camden, NJ, in 1995, and the Ph.D. degree in electrical and computer engineering from the University of Illinois at Urbana-Champaign, Urbana, in 1999.

He has an extensive professional career both in research and industrial research institutions, which includes the following: Research Consultant with Lucent Technologies, Bell Lab, Holmdel, NJ (from 1995 to 1997), R&D Engineer with the Fiber-optics Division, Agilent Technologies (from 1999 to 2001), and R&D Manager with LuxNet Corporation (from 2001 to 2002). Since September 2002, he has been with the National Chiao Tung University, Hsinchu, Taiwan, R.O.C., as a member of the faculty at the Institute of Electro-Optical Engineering. He has authored or coauthored over 60 publications. His current research interests include the epitaxy, design, fabrication, and measurement of high-speed InP- and GaAs-based vertical-cavity surface-emitting lasers, as well as GaN-based light-emitting devices and nanostructures.

Yen-Kuang Kuo was born in Chia-Yi, Taiwan, R.O.C., on July 19, 1959. He received the B.S. degree in electrophysics from National Chiao-Tung University, Hsin Chu, Taiwan, R.O.C., in 1982, the M.S. degree in electrical engineering from National Taiwan University, Taipei, Taiwan, R.O.C., in 1984, and the Ph.D. degree in electrical engineering from University of Southern California (USC), Los Angeles, in 1994.

From 1984 to 1991, he was with the Aeronautical Research Laboratory, Chung Shan Institute of Science and Technology, Taichung, Taiwan, R.O.C. He was a Postdoctoral Research Fellow with the Center for Laser Studies, USC, from 1994 to 1995 where he was engaged in research on passive Q-switching with solid-state saturable absorbers. From 1995 to 1997, he was with the Aerospace Industrial Development Corporation, Taichung, Taiwan, R.O.C. In 1997, he joined the faculty of the Department of Physics, National Changhua University of Education, Changhua, Taiwan, R.O.C., where he is Professor in the Department of Physics and Institute of Photonics, and Head of the Laboratory of Lasers and Optical Semiconductors. His recent research interests include passive Q-switching with solid-state saturable absorbers and semiconductor materials for light-emitting diodes, organic light-emitting diodes, and semiconductor lasers.

Jui-Yen Tsai was born in Hsinchu, Taiwan, R.O.C., in 1972. He received the B.S. degree in physics from Chung Yung Christ University, Chung Li, Taiwan, R.O.C., in 1998, and the M.S. degree from The Institute of Electro-Optical Engineering, National Chiao Tung University (NCTU), Hsinchu, Taiwan, R.O.C., in 2000, where he is currently working towards the Ph.D. degree in the Institute of Electro-Optical Engineering.

From 2000 to 2005, he worked in the Union Optronics corporation as a Senior Research Engineer in epitaxy and process of III–V group materials.

Li-Wen Laih was born in Yurn-Lin Hsien, Taiwan, R.O.C., on September 17, 1970. He received the B.S. degree in electronic engineering from Chung-Yuan Christian University, Chung-Li, Taiwan, R.O.C., in 1994 and the Ph.D. degree in electrical engineering from National Cheng-Kung University, Tainan, Taiwan, R.O.C., in 1997.

He was an Assistant Researcher in Advanced Lab, Chung-Huwa TL, Chung-Li, R.O.C., from 1997 to 2000. He was the VP of R&D in Millennium Communication Co., Ltd., Hsinchu, Taiwan, R.O.C., from 2001 to 2003. He was an Assistant Professor at the Electrical Engineering Department, Chung-Yun Technical University, Chung-Li, R.O.C., from 2004 to 2005. Since October 2006, he has been General Manager in Millennium Communication Co., Ltd. His research are in the field of III–V semiconductor devices including: 1) microwave device: HEMT, FET, HBT; 2) optoelectronic device: vertical-cavity surface-emitting laser (VCSEL), resonant-cavity LED (RCLED), edge-emitting laser (EEL), PIN detector; 3) compound GaAs solar cell. He has over ten years experience on metal–organic chemical-deposition (MOCVD) technology.

Shing-Chung Wang (M'79–SM'03–LM'07) received the B.S. degree in electrical engineering from the National Taiwan University, Taipei, Taiwan, R.O.C., in 1957, the M.S. degree in electrical engineering from the National Tohoku University, Sendai, Japan, in 1965, and the Ph.D. degree in electrical engineering from the Stanford University, Stanford, CA, in 1971.

He has an extensive professional career both in academic and industrial research institutions, which includes the following: member of the faculty at the National Chiao Tung University, Hsinchu, Taiwan (from 1965 to 1967), Research Associate with Stanford University (from 1971 to 1974), Senior Research Scientist with Xerox Corporation (from 1974 to 1985), and Consulting Scientist with Lockheed-Martin Palo Alto Research Laboratories (from 1985 to 1995). Since 1995, he has been a member of the faculty at the Institute of Electro-Optical Engineering, National Chiao Tung University. He has authored or coauthored over 160 publications. His current research interests include semiconductor lasers, vertical-cavity surface-emitting lasers, blue and UV lasers, quantum-confined optoelectronic structures, optoelectronic materials, diode-pumped lasers, and semiconductor-laser applications.

Prof. Wang is a Fellow of the Optical Society of America (OSA) and the recipient of the Outstanding Scholar Award from the Foundation for the Advancement of Outstanding Scholarship.